1. **Title**

The effect of concentration gradients on deflagration-to-detonation transition in a rectangular channel with and without obstructions – a numerical study

2. Authors

Reza Khodadadi Azadboni[a], Ali Heidari[a], Lorenz R. Boeck[b] and Jennifer X. Wen[c]

[a] School of Mechanical & Automotive Engineering, Kingston University London, SW15 3DW, UK

[b] Lehrstuhl für Thermodynamik, Technische Universität München, Garching, 85748, Germany; current address: FM Global, Research Division, Norwood, MA 02062, USA

[c]Warwick FIRE, School of Engineering, University of Warwick, Coventry, CV4 7AL, UK

3. Corresponding author's COMPLETE contact information:

Jennifer Wen (Dr.)

School of Engineering

University of Warwick

Coventry

CV4 7AL, UK

Phone: +44 (0)24 765 73365

Fax: +44 (0)24 76 418922

Email. Jennifer.wen@warwick.ac.uk

Abstract

Explosions in homogeneous reactive mixtures have been widely studied both experimentally and numerically. However, in accident scenarios, mixtures are usually inhomogeneous due to the localized nature of most fuel releases, buoyancy effects and the finite time between release and ignition. It is imperative to determine whether mixture inhomogeneity can increase the explosion hazard beyond what is known for homogeneous mixtures. The present numerical investigation aims to study flame acceleration and transition to detonation in homogeneous and inhomogeneous hydrogen-air mixtures with two different average hydrogen concentrations in a horizontal rectangular channel. A density-based solver was implemented within the OpenFOAM CFD toolbox. The Harten–Lax–van Leer–Contact (HLLC) scheme was used for accurate shock capturing. A high-resolution grid is provided by using adaptive mesh refinement, which leads to 30 grid points per half reaction length (HRL). In agreement with previous experimental results, it is found that transverse concentration gradients can either strengthen or weaken flame acceleration, depending on average hydrogen concentration and channel obstruction. Comparing experiments and simulations, the paper analyses flame speed and pressure histories, identifies locations of detonation onset, and interprets the effects of concentration gradients.

Keywords: *DDT, Detonation, Explosions, Hydrogen, Inhomogeneous mixture*

1. Introduction

While the vast majority of explosions in industry are deflagrations, a worst-case scenario can emerge if transition from deflagration to detonation occurs during an explosion. Deflagrations require congestion and confinement to generate significant overpressures; by contrast, detonations inherently produce high overpressure and have the potential to propagate across large unobstructed and unconfined distances without substantial weakening.

Thomas [3] gave a comprehensive discussion on various mechanisms of deflagration-to-detonation transition (DDT) and differentiated the terminology between global DDT and local DDT. Global DDT includes both flame acceleration (FA) and the onset of detonation. Local DDT refers to the actual onset of detonation at the location where the combustion mechanism changes from diffusion-controlled to auto-ignition controlled. In this work, the term DDT is used in the global sense and includes both FA and the onset of detonation.

While DDT in homogeneous mixtures has been widely investigated [4], fewer studies have addressed the effect of spatial gradients in mixture composition. Kuznetsov et al. [5] conducted large-scale experiments of FA and DDT in an obstructed semi-confined flat layer of hydrogen-air mixture with transverse (vertical) concentration gradients. The authors found that DDT propensity is increased by mixture inhomogeneity for globally lean mixtures, and may be correlated with the maximum local hydrogen concentration within the layer. Vollmer et al. [6] and Boeck et al. [7-9] reported a strong effect of concentration gradients on FA and DDT in an entirely closed channel at laboratory-scale. Boeck et al. observed that in a channel with obstructions, concentration gradients promoted FA and DDT only in globally lean mixtures with an average hydrogen concentration

below about 24%; for richer mixtures, the presence of gradients lead to weaker FA and delayed DDT. The authors proposed that a mixture-averaged flame speed parameter (σS_L) may predict this effect, taking into account the integral rate of combustion and expansion which drives flame acceleration in a closed channel. By contrast, for unobstructed channels, gradients always led to stronger FA and earlier DDT, independent of the average hydrogen concentration; this was attributed to flame surface area enlargement driven by concentration gradients.

The present work aims at extending the existing physical understanding of deflagration-to-detonation transition in hydrogen-air mixtures with transverse concentration gradients in closed channels. Since extensive knowledge on these processes has been built up over decades for homogeneous mixtures, the approach is to identify similarities and differences caused by concentration gradients compared to homogenous mixtures with equal average hydrogen concentration. This work numerically investigates four cases that were studied experimentally by Boeck et al. [2]. Experimental data is used for model validation, and novel insight is gained from the simulations that could not be obtained from the experiments: continuous histories of pressure and flame location and speed are produced, as well as fields of density and pressure which reveal the mechanisms of flame acceleration and onset of detonation.

2. The experiments considered

DDT experiments of Boeck et al. [2] are considered which compare homogeneous and inhomogeneous hydrogen-air mixtures in terms of flame speed and overpressure. The experiments were conducted in a horizontal channel with and without internal obstructions. As shown in Fig. 1, the channel measured 5.4 m (L) × 0.3 m (W) × 0.06 m (H). One obstructed configuration is

considered: seven flat-plate obstacles with a blockage ratio of 60% (BR60) were placed in a region 0.25 m < x < 2.05 m from the ignition location at the left end of the channel with an obstacle spacing of 0.3 m while the remaining channel length was unobstructed. In addition, an unobstructed configuration (BR00) is considered where all obstacles were removed. Concentration gradients as shown in Figure 2 were generated by gas injection through the channel top plate, formation of a hydrogen layer near the channel ceiling, and subsequent diffusion. The gradients were oriented vertically, thus perpendicular to the main direction of flame propagation. The mixture was ignited by a weak electric spark centered at x = 0 m. Measurements were conducted for flame-tip velocity using photodiodes, obtaining local flame speed by linear interpolation between arrival times, and overpressure using piezo-electric pressure transduces at the channel ceiling. See [2] for further details on the experiment and diagnostics.

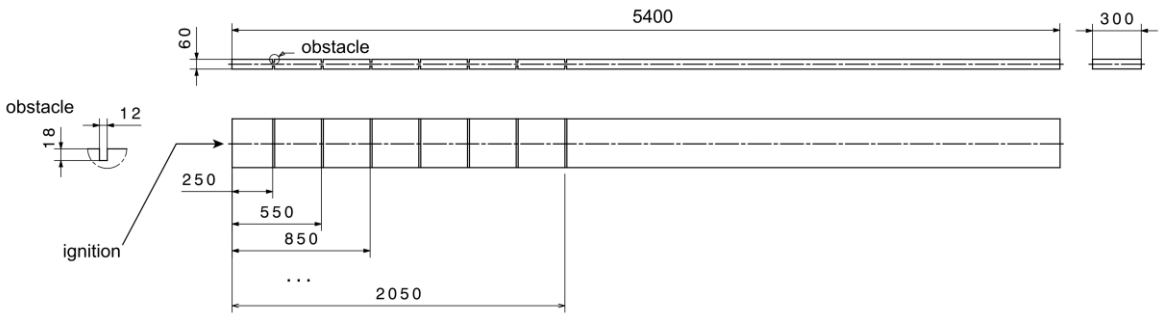

Fig. 1. Geometry of the explosion channel, obstructed configuration (BR60). Dimensions in (mm).

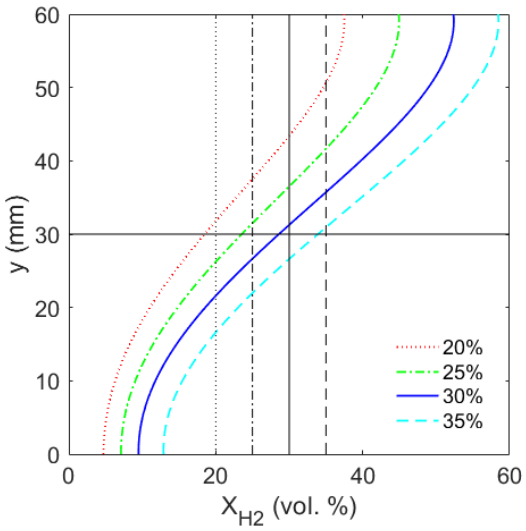

Fig. 2. Hydrogen concentration profiles across the channel height for different average hydrogen concentrations [2].

As summarized in Table 1, a total of eight conditions were simulated for different hydrogen concentrations with both homogeneous and inhomogeneous mixtures with and without obstructions.

Table 1
Test conditions numerically simulated

Hydrogen concentration (%)	**Homogeneous**		**Inhomogeneous**	
	Unobstructed	Obstructed	Unobstructed	Obstructed
20		✓		✓
25	✓		✓	
30		✓		✓
35	✓		✓	

3. Numerical methodology

A density-based solver, VCEFoam, which has been assembled by the authors [10-12] within the framework of the open source CFD code OpenFOAM [13], is used with the Monotone Integrated Large Eddy Simulation (MILES) approach. Within VCEFoam, compressible Navier–Stokes equations with a hydrogen-air reaction mechanism which contains 9 species and 21 detailed reactions [14] are solved. The HLLC (Harten-Lax-van Leer-Contact) [15] for shock capturing and the Runge-Kutta scheme [16] for the time discrete schemes, which includes the dual time scheme and the physical time step. The solver and numerical schemes have been previously tested by solving the Sod's shock tube problem [1, 10].

4. Numerical setup

The two-dimensional computational domain was constructed identical to the experiment geometry. Initial pressure and temperature were 101.33 kPa and 293 K, respectively. Weak ignition was modeled by imposing a temperature of 2300 K at initial pressure in a patch of cells with a radius of 10 mm around the ignition point (x = 0 m, y = 0.03 m).

In the present simulations, the half-reaction length (HRL) varies across the domain due to inhomogeneous mixture composition, between 30 and 50 grid points per HRL (1/HRL). This resolution exceeds the resolution of previous 2-D DDT simulations in the literature [17-20]. Sharpe [18] observed that the results for grid resolutions above 20 1/HRL are sufficient. The present geometry is significantly larger than widely simulated mm-scale channels and a resolution higher than what was used here would exceed presently available computational resources. Mesh sensitivity and validation can be found in previous publications [10-11]. In this study, adaptive

mesh refinement was used to provide a minimum cell size of 10 μm, equivalent to a minimum of 30 grid points per half-reaction length.

5. Results

This section presents results from simulations of cases defined in Table 1. Simulated flame speed and pressure data are compared against experiments available online [2], and OH-PLIF images [2] are used to substantiate numerical results in terms of flame topology. Additional flow field parameters from the numerical simulations are analysed to extend the interpretation of concentration gradient effects on FA and DDT.

5.1 Obstructed channel

The following sections present results in the obstructed channel for mixtures with average hydrogen concentrations of 30% and 20%.

5.1.1 30% hydrogen concentration (near-stoichiometric mixture)

Figure 3 shows flame speed data from experiments and simulations with 30% hydrogen-air mixtures in the obstructed channel (BR60). In addition to photodiodes, pressure transducers were used for experimental velocity measurements in the detonation regime. For both homogeneous and inhomogeneous mixtures, the flame tip velocity initially rises monotonically in the obstructed part of the channel (0 m < x < 2.05 m) and reaches values around 2000 m/s, indicating transition to detonation within the obstructed channel section. It is difficult to determine the precise location of the onset of detonation solely from flame speed measurements due to insufficient resolution. Initial FA is slightly stronger in the homogeneous mixture compared to the inhomogeneous mixture. The simulated flame tip velocities are in reasonably good agreement with the measurements.

Pressure histories from experiments and simulations at are compared in Fig. 4 at a transducer location of x = 1.4 m. The pressure history for the homogeneous mixture shows a sharp increase in pressure at t = 12.4 ms to its peak value; by contrast, the inhomogeneous mixture shows an initial pressure increase at t = 11.4 ms to about 14 bar, a subsequent short decrease, and a secondary sharp increase to its peak value of about 30 bar at t = 11.5 ms. The step-wise increase in pressure and high secondary peak pressure observed for the inhomogeneous mixture suggests that the onset of detonation occurred in the immediate vicinity of the pressure transducer, at x = 1.4 m. By contrast, the single pressure increase observed for the homogeneous mixture suggests that the onset of detonation has occurred earlier, upstream of the transducer, and a detonation wave passes the transducer. These initial observations are supported in the following by analysis of numerical schlieren sequences.

Figure 5 shows numerical schlieren sequences for both homogeneous (left) and inhomogeneous mixture (right). It can be seen, that the concentration gradients affect the flame shape and also the formation of leading shock waves and vortices downstream of the obstacles. In both cases, local DDT is initiated by precursor-shock reflection at the upstream faces of an obstacle, leading to local explosions behind the reflected shock wave and an over-driven detonation wave which eventually decays toward the Chapman-Jouguet state. For the homogeneous mixture, secondary hot-spots are generated downstream of the obstacle which accomplishes the onset near the centre axis of the channel. At 12.39 ms, precursor shock waves are seen in front of the flame. The following frames show strong acceleration of the flame towards the precursor shocks and, eventually, the formation of a detonation wave. For the inhomogeneous mixture, local explosions at the upstream obstacle face directly cause the onset of detonation at 11.485 ms. In the homogeneous mixture onset occurs

between obstacles, at x = 1.3 m, whereas in the inhomogeneous mixture, the onset takes place slightly later, at the obstacle at x = 1.45 m, which is consistent with initial observations from experimental and simulated flame speed and pressure histories.

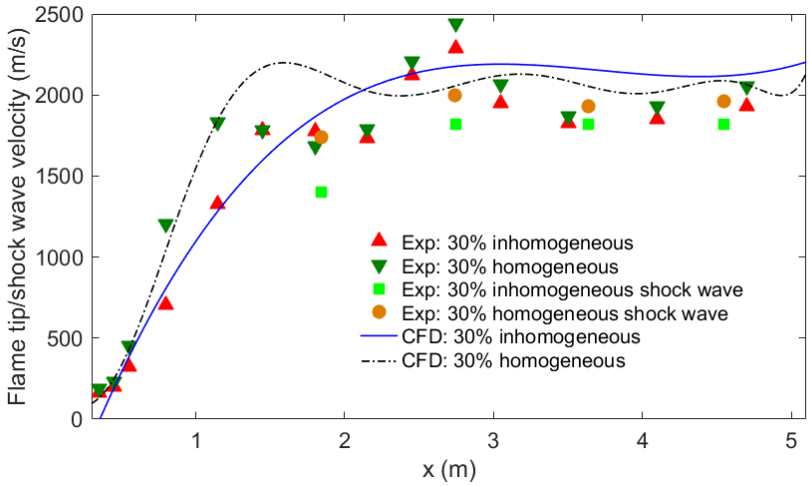

Fig. 3. Comparison of the flame tip velocities between homogeneous and inhomogeneous mixtures with 30% hydrogen concentration (BR60). Experimental data (markers) and numerical predictions (lines).

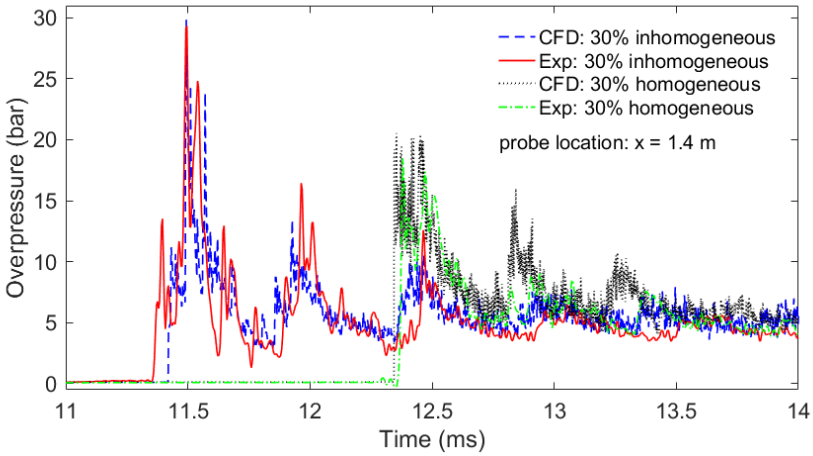

Fig. 4. Comparison of overpressure at x = 1.4 m between the homogeneous and inhomogeneous mixtures at 30% hydrogen concentration (BR60).

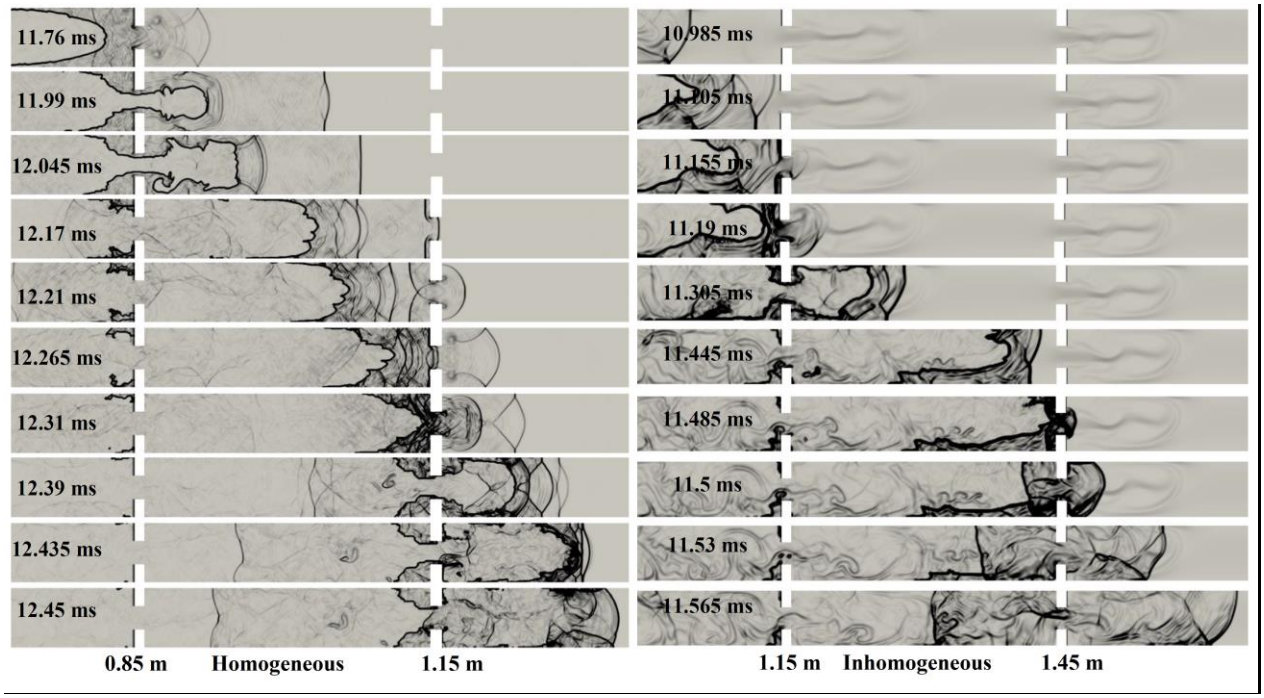

Fig. 5. Numerical schlieren fields for 30% hydrogen concentration (BR60). (Left: homogeneous mixture; right: inhomogeneous mixture).

Figure 5 demonstrates that, even for symmetric initial conditions in the case of a homogeneous mixture, an asymmetric flow field and flame shape can develop. Such asymmetry is commonly observed in simulations of flame propagation in tubes with hydrogen-air mixtures due to (1) high sensitivity of flame instabilities to perturbations at the level of numerical accuracy; and (2) the effect of gravity which is included in the present simulations.

In reacting flows with strong density and pressure gradients, including deflagrations, detonation waves, and DDT processes, hydrodynamic instabilities are one of the key factors in enhancing turbulence through shock-flame interaction [12]. The main hydrodynamic instabilities in these phenomena are; Kelvin Helmholtz (KH) instability, which manifests itself as small-scale vortices on the flame shear layer, and Richmeyer Meshkov (RM) instability appear as mushroom-shaped forward/backward jets with steep gradients in pressure and density [12]. These hydrodynamic instabilities are identified in Fig. 6.

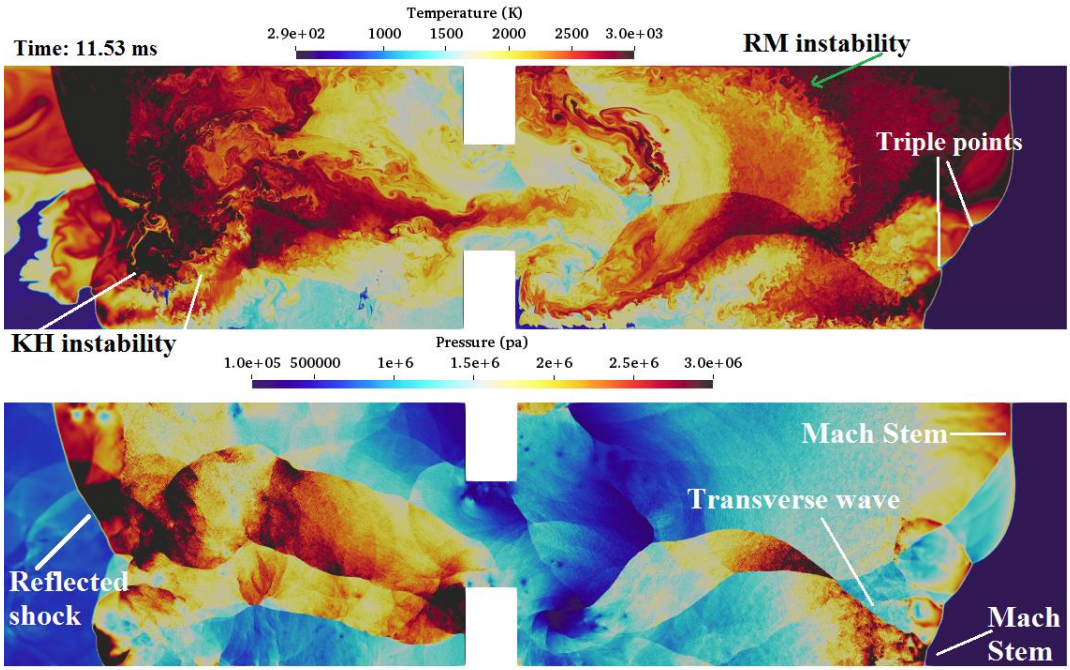

Fig. 6. Small-scale features: temperature (top) and pressure (bottom) fields for the inhomogeneous mixture with 30% average hydrogen concentration. The obstacle in the field of view (FOV) is located at x = 1.45 m; time = 11.53 ms.

5.1.2 20% hydrogen concentration (lean mixture)

Figure 7 shows flame speed data from experiments and simulations with 20% hydrogen-air mixtures in the obstructed channel. In contrast to the 30% case, FA is stronger in the obstructed channel section for the inhomogeneous mixture compared to a homogeneous mixture. The difference is small but discernible in the obstructed channel section both in experiments and simulations. In the unobstructed section, the flame speed plateaus in the homogeneous mixture whereas it keeps increasing in the inhomogeneous case. This steady acceleration in the unobstructed channel section in the inhomogeneous mixture was attributed to continuous enlargement of the flame surface area due to the concentration gradient [7,8] and is captured in the numerical simulation. This effect will be revisited in more detail later for the entirely unobstructed channel. A sudden increase in flame tip velocity at $x \approx 4$ m indicates transition to detonation in the simulation. This was not visible as clearly in the measurements, where a more gradual increase in flame speed to 1700 m/s was measured towards the channel end. The large spacing of photodiodes used for velocity measurements in this region could not resolve sharp changes in the flame speed so that it is not entirely clear whether DDT occurred in the experiment.

Figure 8 presents pressure histories from experiments and simulations taken at $x = 4.1$ m. Pressure traces show the substantial difference in explosion violence between the homogeneous and inhomogeneous mixture, with peak pressure for the inhomogeneous mixture more than twice as high as for the homogeneous mixture. It can be seen, that the overpressure in the inhomogeneous case exceeds Chapman-Jouguet (CJ) pressure, which is around 14 bar, which suggests that transition to detonation has occurred upstream of the pressure measurement location. The second pressure increase at $t = 21$ ms represents the reflected wave from the channel end plate. By contrast,

comparably low overpressure in case of the homogeneous mixture with a sharp initial pressure increase suggests that a fast deflagration passes the pressure transducer in this case.

Figure 9 presents numerical pressure and schlieren fields of detonation onset in the inhomogeneous mixture. The leading flame tip is initially located near the channel top wall, and the flame is elongated due to the concentration gradient providing highest local mixture reactivity near the channel ceiling. A local explosion is observed near the leading flame tip, initiating the onset of detonation and driving a shock wave diagonally forward toward the channel bottom. This process is in qualitative agreement with the experimental observations in unobstructed channels and mixtures with concentration gradients [2,7].

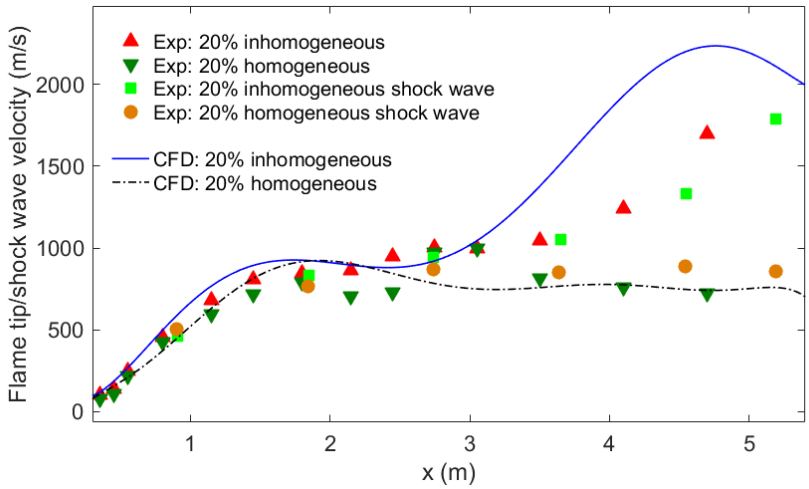

Fig. 7. Comparison of the flame tip velocities between homogeneous and inhomogeneous mixtures with 20% hydrogen concentration (BR60). Experimental data (markers) and numerical predictions (lines).

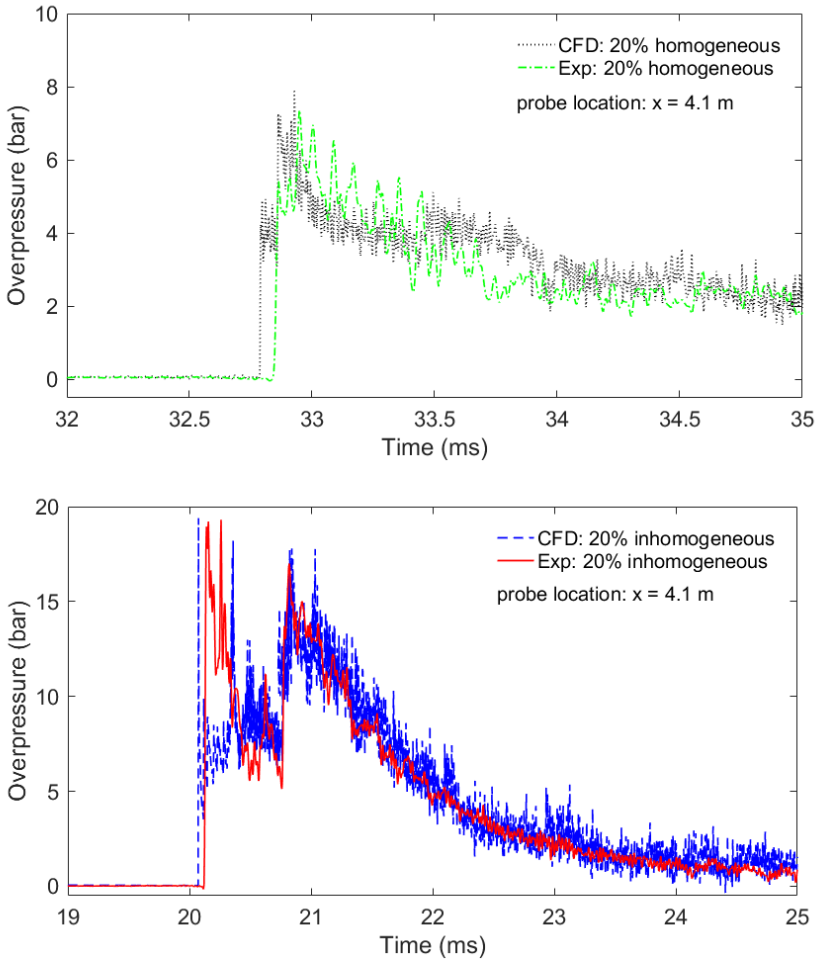

Fig. 8. Comparison of overpressure at x = 4.1 m between the homogeneous (top) and inhomogeneous (bottom) mixtures at 20% hydrogen concentration (BR60).

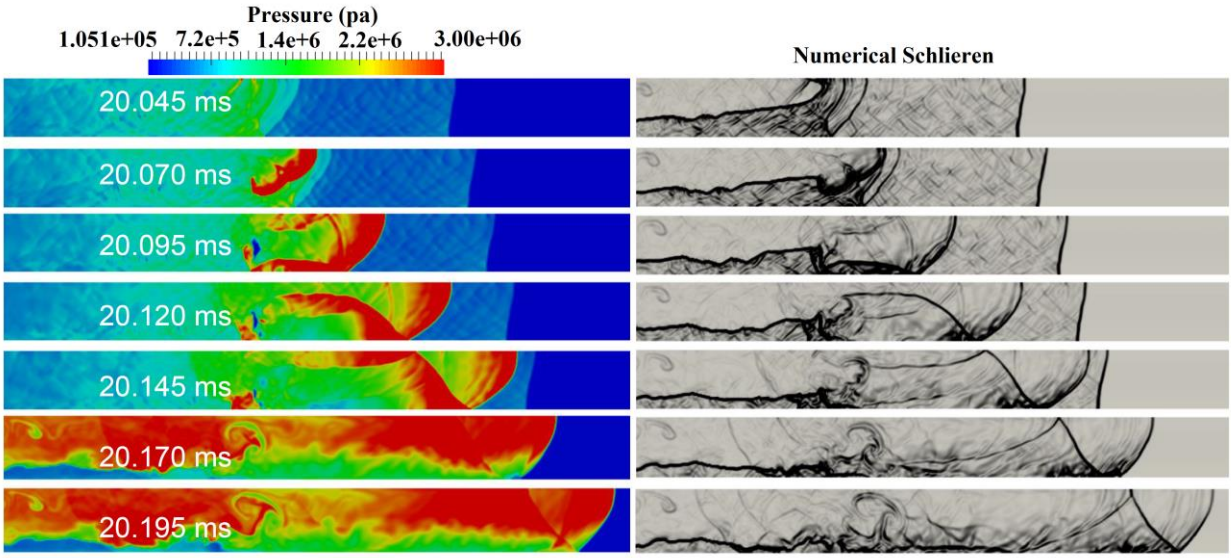

Fig. 9. Pressure (left) and numerical schlieren (right) fields of detonation onset in the inhomogeneous 20% hydrogen-air mixture. The field-of-view extends from x = 3.75 m to x = 4.16 m.

5.2 Unobstructed channel

The following sections present results on FA and DDT in the unobstructed channel for mixtures with average hydrogen concentrations of 25% and 35%.

5.2.1 Mixture of 25% hydrogen concentration (lean mixture)

Figure 10 shows flame speed data from experiments and simulations with 25% hydrogen-air mixtures in the unobstructed channel. FA in the inhomogeneous mixture is significantly stronger than FA in the homogeneous mixture and allows for DDT near the end of the channel. By contrast, FA is weak in the homogeneous mixture, resulting in a slow deflagration throughout the entire channel. Both cases are well reproduced by the numerical simulations.

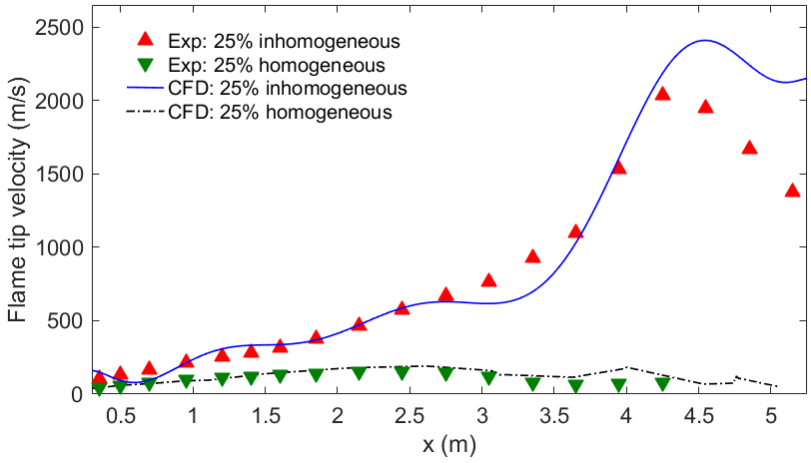

Fig. 10. Comparison of the flame tip velocities between homogeneous and inhomogeneous mixtures with 25% hydrogen concentration (BR00). Experimental data (markers) and numerical predictions (lines).

Figure 11 presents pressure histories from experiments and simulations taken at x = 5 m. These pressure histories illustrate the substantial difference in explosion violence between the homogeneous and inhomogeneous mixture: pressure remains low for the homogeneous mixture, and there are no signatures of strong shock waves, indicative of a slow deflagration; the inhomogeneous mixture shows detonation at the pressure transducer location.

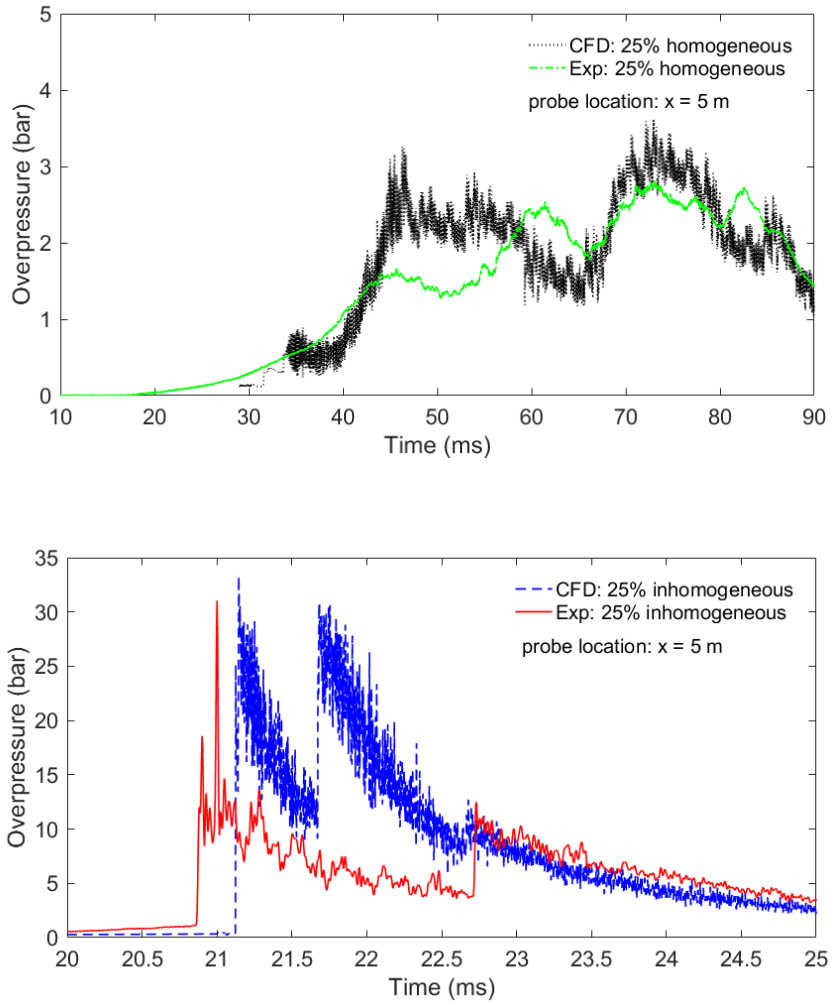

Fig. 11. Comparison of overpressure at x = 5 m between the homogeneous (top) and inhomogeneous (bottom) mixtures at 25% hydrogen concentration (BR00).

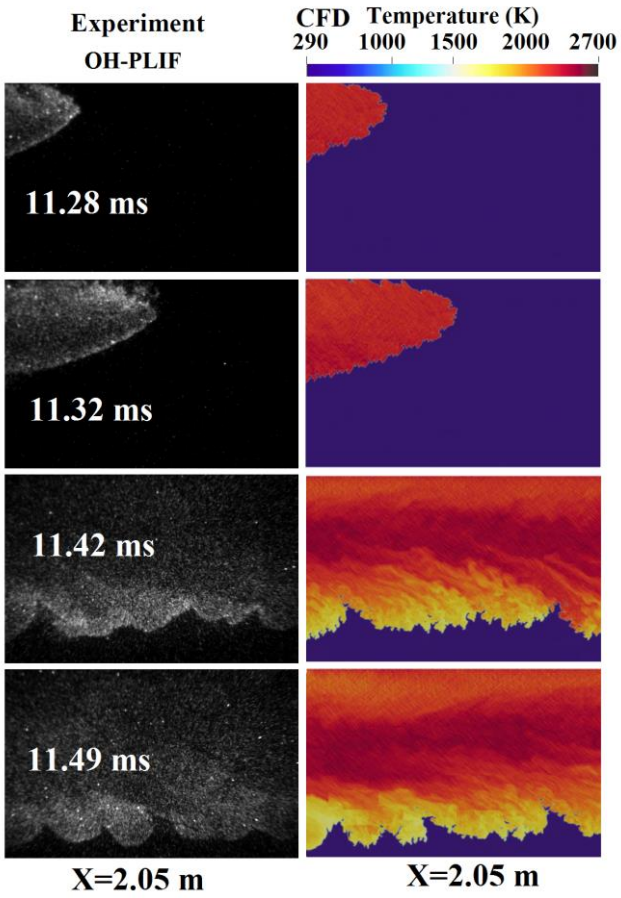

Fig. 12. Sequence of flame propagation, inhomogeneous 25% hydrogen-air (BR00) (Left: OH-PLIF measurements; Right: the predicted temperature fields).

Figure 12 shows a qualitative comparison between experimental OH-PLIF images of the leading flame edge [2] and numerical temperature fields at x = 2.05 m. The leading edge of the flame propagates along the channel top wall, in the region of maximum mixture reactivity, and the overall surface area of the flame is significantly enlarged compared to a symmetric convex flame which occurs in homogeneous mixtures, leading to increased global heat release rate and faster flame acceleration. This geometric effect supports strong FA in mixtures with concentration

gradients in the unobstructed channel. Wrinkling of the flame front facing the channel floor is observed; it is unclear whether this is due to intrinsic flame instabilities or flow instability related to the gradients in the horizontal flow velocity ahead of the flame.

5.2.2 Mixture of 35 % hydrogen concentration (rich mixture)

Figure 13 shows flame speed data from experiments and simulations with 35% hydrogen-air mixtures in the unobstructed channel. FA is slightly stronger in the inhomogeneous mixture than in the homogeneous mixture; DDT occurs in both mixtures near the end of the channel. Overall, the difference in explosion violence between homogeneous and inhomogeneous mixture is less significant than previously observed for the 25% hydrogen-air mixture, where the concentration gradient caused a difference in combustion regime.

Figure 14 presents pressure histories from experiments and simulations taken at x = 5 m. The high peak pressure for the homogeneous mixture, on the order of 100 bar, indicates that onset of detonation occurred near the transducer location. Such high peak pressures are related to the over-driven detonation state immediately after detonation onset, and to multi-dimensional reflections at the transducer location. Onset occurred earlier (x < 5 m) in the inhomogeneous mixture, resulting in a detonation propagating past the transducer with a peak pressure closer to CJ pressure.

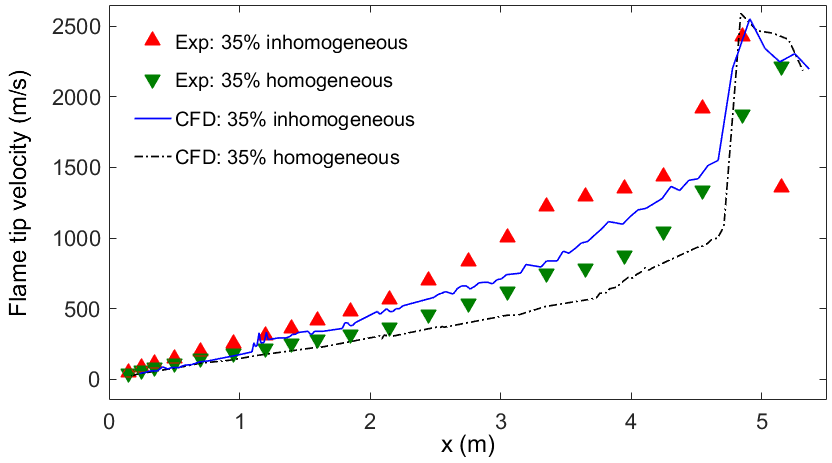

Fig. 13. Comparison of the flame tip velocities between homogeneous and inhomogeneous mixtures with 35% hydrogen concentration (BR00). Experimental data (markers) and numerical predictions (lines).

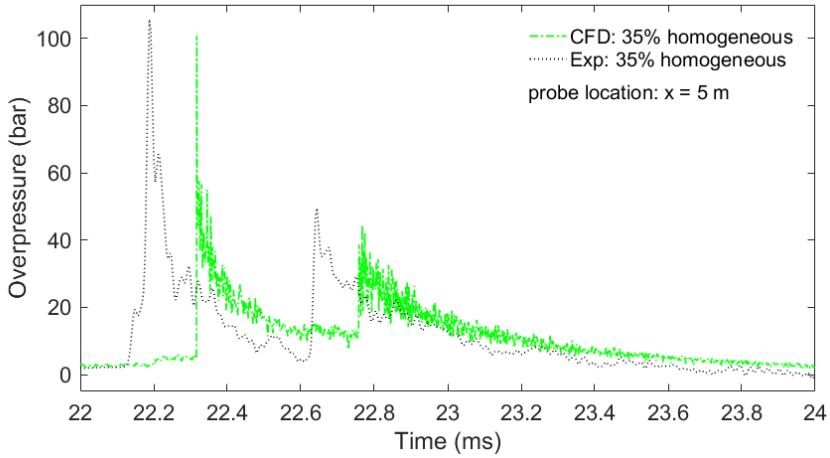

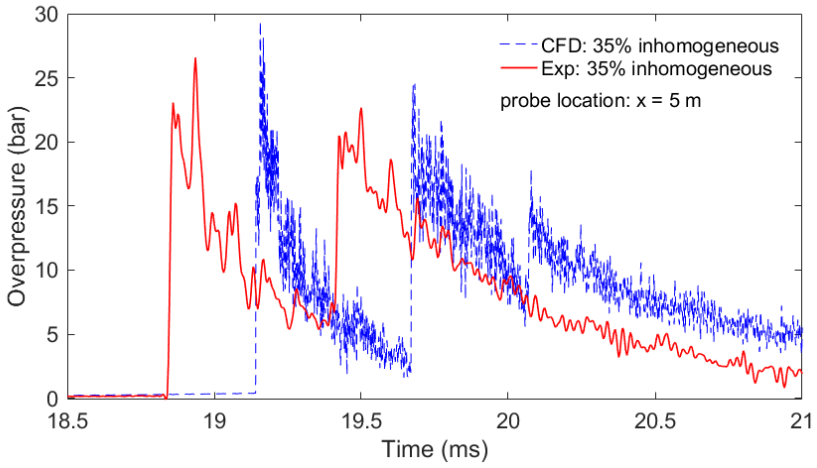

Fig. 14. Comparison of overpressure at x = 5 m between the homogeneous (top) and inhomogeneous (bottom) mixtures at 35% hydrogen concentration (BR00).

6. Discussion

Results from numerical simulations presented in Sec. 5 demonstrate that transverse gradients in hydrogen concentration can either promote or weaken FA and lead to earlier or delayed transition to detonation. Previous experiments have revealed this effect of gradients on FA clearly; however, the effect on run-up distances to DDT was captured less accurately: for precise experimental measurements of DDT location, optical high-speed video is needed, but optical access to the channel was limited to an optical segment providing access to one location at a time. Onset of detonation can be identified in the numerical simulations based on a sudden rise in peak pressure within the domain.

Table 2 summarizes DDT locations for the simulated obstructed channel configurations. For a hydrogen concentration of 20%, DDT occurred only for the inhomogeneous mixture. Flame speeds were similar for homogeneous and inhomogeneous mixtures at the end of the obstructed section, x

= 2.05 m, and a strong effect of mixture inhomogeneity occurred after flame transition into the unobstructed channel section. The obstacles effectively reduced flame elongation within the obstructed channel region, and elongation took place subsequently in the unobstructed region. For a hydrogen concentration of 30%, mixture inhomogeneity led to weaker FA and slightly delayed DDT within the obstructed channel section.

Table 2
Summary of transition to detonation in the obstructed channel

Hydrogen concentration	**Homogeneous**	**Inhomogeneous**
20 %	No DDT (maximum flame speed = 950 m/s)	DDT at x = 3.9 m
30 %	DDT at x = 1.3 m	DDT at x = 1.45 m

Table 3 provides a summary of phenomena observed in the numerical simulations and experiments in the unobstructed channel configuration. It can be seen that, in the unobstructed channel with the homogeneous mixtures, DDT only occurs in highly reactive mixtures with high burning velocity such as 35% hydrogen. However, for inhomogeneous mixtures, the transition to detonation occurs even in a globally lean mixture such as 25%.

FA becomes stronger with increasing hydrogen concentration, both for homogeneous and inhomogeneous mixtures; however, the distance to DDT in inhomogeneous mixtures increases with increasing average hydrogen concentration. Figure 12 reveals that transition to detonation occurs at a higher flame speed in the inhomogeneous mixture compared to the homogeneous mixture.

Table 3
Summary of transition to detonation in the unobstructed channel

Hydrogen concentration	**Homogeneous**	**Inhomogeneous**
20 %	No DDT (maximum flame speed = 45 m/s)	No DDT (maximum flame speed = 200 m/s)
25 %	No DDT (maximum flame speed = 150 m/s)	DDT at x = 4.55 m
30 %	No DDT (maximum flame speed = 1000 m/s)	DDT at x = 4.6 m
35 %	DDT at x = 4.9 m	DDT at x = 4.78 m

Boeck et al. [7,8] proposed an integral reactivity parameter $(S_L\sigma)_{eff}$ for non-uniform mixtures which captures the effect of concentration gradient of FA:

$$(S_L\sigma)_{eff} = \int_0^H [S_L(y)\sigma(y)]dy. \quad (1)$$

For average hydrogen concentrations below about 24%, mixtures with concentration gradients exhibit larger $(S_L\sigma)_{eff}$ than homogeneous mixtures with equal average hydrogen concentration. For average hydrogen concentrations greater than 24%, homogeneous mixtures yield higher $(S_L\sigma)_{eff}$, independent of the shape of the concentration gradient profile, as long as the profile is symmetric to the centre axis of the channel. Since flame elongation effects are largely suppressed in the obstructed channel, s. Fig. 5, the effect of effective flame speed $(S_L\sigma)_{eff}$ dominates the overall effect of concentration gradients on FA. By contrast, for the unobstructed channel, gradients cause stronger FA for all average hydrogen concentrations investigated, due to strong flame elongation and increase in flame surface area, s. Fig. 8. For further details on the concept of integral reactivity of inhomogeneous mixtures see [7,8].

7. Conclusions

Numerical studies were conducted to investigate flame acceleration and transition to detonation in both homogeneous and inhomogeneous hydrogen-air mixtures in obstructed and unobstructed channel configurations. A density-based solver within the OpenFOAM toolbox was used. The numerical predictions were compared against previous experiments and numerically predicted flame tip velocities, pressure histories and locations of detonation onset were in reasonably good agreement with the measurements.

This study substantiates previous experimental observations that transverse concentration gradients in channels can lead to either stronger or weaker FA and higher or lower propensity for DDT, depending on the geometrical channel configuration and mixture composition, in comparison with homogeneous mixtures with the same average hydrogen concentration. For the obstructed channel, gradients promoted FA only in mixtures with average hydrogen concentrations below about 24% for the conditions studied in this work, whereas gradients in richer mixtures weakened FA. By contrast, gradients promoted FA irrespective of average hydrogen concentration in the unobstructed channel. Flames in mixtures with concentration gradients are observed to elongate while propagating through the unobstructed channel, which enlarges the flame surface area, increases the integral rate of combustion, and promotes FA.

It is critical to realize that unobstructed geometries, which are typically associated with a low potential for strong FA and long run-up distances to DDT due to the lack of congestion, can indeed exhibit strong FA and early DDT when concentration gradients are present. Further work is needed to establish quantitative guidance for explosion protection in the presence of concentration gradients, and to integrate the integral reactivity approach into predictive models for FA and DDT

for closed channels and pipes. Numerical simulations can substantially support the interpretation of experiments and provide detailed insight into local phenomena.

Acknowledgement

Reza Khodadadi Azadboni is funded by through the Innovative Doctoral Programme (IDP) "Numerical characterization and simulation of the complex physics underpinning the Safe Handling of Liquefied Natural Gas (SafeLNG)" (2014-2017) funded by the Marie Curie Action of the 7th Framework Programme of the European Union.

References

[1] Sod GA. A survey of several finite difference methods for systems of nonlinear hyperbolic conservation laws. J Comput Phys 1978; 27:1–31.

[2] Boeck LR, Katzy P, Hasslberger J, Kink A, Sattelmayer T. The "GraVent DDT Database". Shock Waves 2016; 26:683–685.

[3] Thomas GO. Some observations on the initiation and onset of detonation. Philos Trans A Math Phys Eng Sci 2012; 370:715–39.

[4] Ciccarelli G, Dorofeev SB. Flame acceleration and transition to detonation in ducts. Prog Energy Combust Sci 2008; 34:499-550.

[5] Kuznetsov MS, Grune J, Friedrich A, Sempert K, Breitung W, Jordan T. Hydrogen-air deflagrations and detonations in a semi-confined flat layer. In Sixth International Seminar on Fire and Explosion Hazards 2011; p. 978–981.

[6] Vollmer KG, Ettner F, Sattelmayer T. Deflagration-to-detonation transition in hydrogen-air mixtures with a concentration gradient. Combust Sci Technol 2012; 184:1903–1915.

[7] Boeck LR. Deflagration-to-detonation transition and detonation propagation in H_2-air mixtures with transverse concentration gradients. Ph.D. Thesis, Technical University of Munich, 2015.

[8] Boeck LR, Hasslberger J, Sattelmayer T. Flame acceleration in hydrogen/air mixtures with concentration gradients. Combust Sci Technol 2014; 186:1650–1661.

[9] Boeck LR, Berger FM, Hasslberger J, Sattelmayer T. Detonation propagation in hydrogen–air mixtures with transverse concentration gradients. Shock Waves 2015; 26:181–192.

[10] Khodadadi Azadboni R, Wen JX, Heidari A, Muppala SPR, Wang CJ. Numerical modeling of deflagration to detonation transition in inhomogeneous hydrogen/air mixtures. J Loss Prev Process Ind 2017; 49:722-730.

[11] Khodadadi Azadboni R, Wen JX, Heidari A. In: Nóbrega JM, Jasak H, editors. OpenFOAM®: Selected papers of the 11th Workshop, Springer, 2017. ISBN: 9783319608457.

[12] Khodadadi Azadboni R, Heidari A, Wen JX. A computational fluid dynamic investigation of inhomogeneous hydrogen flame acceleration and transition to detonation. Flow Turbul Combust 2018; 1–13.

[13] OpenFOAM Ltd., OpenFOAM, Available from: http://www.openfoam.com/

[14] O'Conaire M, Curran H, Simmie J, Pitz W, Westbrook C. A comprehensive modeling study of hydrogen oxidation. Int J Chem Kinet 2004; 36:603-622.

[15] Batten P, Leschziner MA, Goldberg UC. Average-state Jacobians and implicit methods for compressible viscous and turbulent flows. J Comput Phys 1997; 137:38–78.

[16] Borm O, Jemcov A, Kau HP. Density based Navier Stokes solver for transonic flows. In: Proceedings of 6th OpenFOAM workshop, Penn State University, USA, 2011.

[17] Gamezo VN, Ogawa T., Oran ES. Numerical simulations of flame propagation and DDT in obstructed channels filled with hydrogen-air mixture. Proc Combust Inst 2007;31: 2463-2471.

[18] Ogawa T, Oran ES, Gamezo VN. Numerical study on flame acceleration and DDT in an inclined array of cylinders using an AMR technique. Computers Fluids 2013; 85:63-70.

[19] G. J. Sharpe. Transverse waves in numerical simulations of cellular detonations. J Fluid Mech 2001;447: 31–51.

[20] Emami S, Mazaheri K, Shamooni A, Mahmoudi Y. LES of flame acceleration and DDT in hydrogen-air mixture using artificially thickened flame approach and detailed chemical kinetics. J Hydrogen Energy 2015; 40:7395-7408.